doi:10.1016/j.jmb.2004.03.020 J. Mol. Biol. (2004) 338, 839–846

JMB

Available online at www.sciencedirect.com

SCIENCE DIRECT®

ELSEVIER

A Mutant KcsA K^+ Channel with Altered Conduction Properties and Selectivity Filter Ion Distribution

Ming Zhou and Roderick MacKinnon*

Howard Hughes Medical Institute and Laboratory of Molecular Neurobiology and Biophysics, Rockefeller University, New York NY 10021, USA

The selectivity filter of K^+ channels is comprised of a linear queue of four equal-spaced ion-binding sites spanning a distance of 12 Å. Each site is formed of eight oxygen atoms from the protein. The first three sites, numbered 1–3 from the extracellular side, are made of exclusively main-chain carbonyl oxygen atoms. The fourth site, closest to the intracellular side, is made of four main-chain carbonyl oxygen atoms and four threonine side-chain hydroxyl oxygen atoms. Here we characterize the effects of mutating the threonine to cysteine on the distribution of ions in the selectivity filter and on the conduction of ions through the filter. The mutation influences the occupancy of K^+ at sites 2 and 4 and it reduces the maximum rate of conduction in the limit of high K^+ concentration. The mutation does not affect the conduction of Rb^+. These results can be understood in the context of a conduction mechanism in which a pair of K ions switch between energetically balanced 1,3 and 2,4 configurations.

Keywords: potassium channel; permeation; selectivity filter; ion occupancy; single channel current

*Corresponding author

Introduction

Potassium channels conduct K ions very rapidly across the cell membrane. In the presence of physiological electrochemical differences, K ions are conducted across the membrane almost as fast as they are able to diffuse from solution up to the pore entryway. The mechanism of this rapid conduction is very interesting to understand, especially since K^+ channels exclude the smaller alkali metal cation Na^+. Here we ask how a mutation at a single site in the selectivity filter influences the occupancy distribution and conduction of ions in the KcsA K^+ channel. Our aim is to test a specific mechanism that has been proposed to underlie ion conduction.

In the K^+ selectivity filter the amino acid sequence TVGY forms an extended strand that directs the threonine hydroxyl oxygen and four carbonyl oxygen atoms toward the ion conduction pore (Figure 1A). Four strands (one from each subunit) come together to create five layers of four in-plane oxygen atoms; half way between each layer a K^+ interacts favorably with eight oxygen atoms, four from each adjacent layer. These favorable positions, or K^+ binding sites, are labeled 1–4 from the extracellular to the intracellular side of the selectivity filter.

Under physiological K^+ concentrations, on average, two K ions reside in the selectivity filter at a given time. This conclusion was most definitively reached through crystallographic analysis at 1.9 Å resolution of a KcsA K^+ channel structure containing Tl^+ substituted for K^+.[1] The two K ions in the filter have been proposed to reside in specific configurations called 1,3 and 2,4, referring to K^+ being at sites 1 and 3 and at 2 and 4, respectively. In both configurations a water molecule is thought to reside in between the pair of ions. Evidence for these specific configurations comes from a structural comparison of Rb^+ and K^+ in the selectivity filter[2] and from a characteristic feature of electron density at the selectivity filter entryway in the presence of K^+.[3]

The 1,3 and 2,4 configurations suggest a simple throughput cycle for the conduction of K^+ (Figure 1B). The configurations are able to interchange when the queue of ions and water simply shifts from one configuration to the other or when an ion enters from the ion vacant side of the filter (i.e.

E-mail address of the corresponding author: mackinn@mail.rockefeller.edu

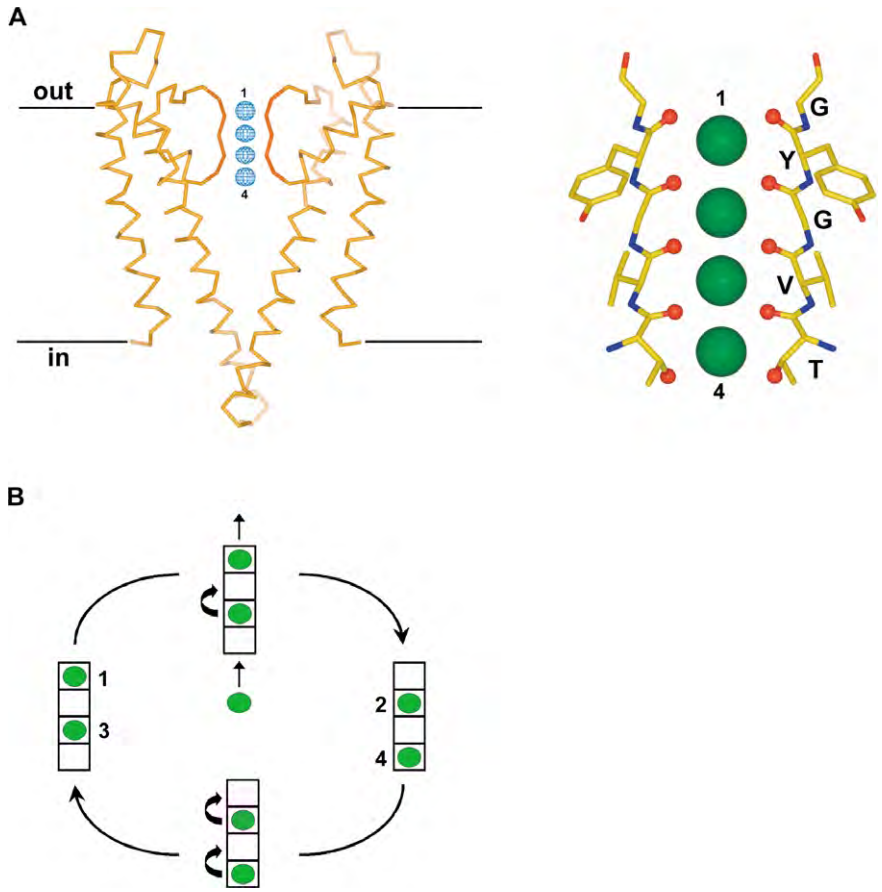

Figure 1. A, Ion-binding sites in the selectivity filter of KcsA (modified from Figure 1 of Zhou & Mackinnon[1]). Left, overview of ion-binding sites in the selectivity filter. The black lines indicate the external and internal membrane surfaces. Two diagonally opposed subunits of the tetrameric channel are shown as a yellow trace. The selectivity filter, residues T75 to G79, is colored in red. The $F_o - F_c$ omit map (contoured at 3σ) validating the K^+ sites is shown as a blue mesh with sites 1 and 4 labeled. Right, close-up view of the selectivity filter region (T75 to G79) in a ball-and-stick representation. The four K^+ binding sites in the selectivity filter are represented as green spheres with sites 1 and 4 labeled. B, A simplified throughput cycle for K^+ conduction (modified from Morais-Cabral *et al.*[2]). Sets of boxes represent the four K^+ binding sites within the selectivity filter. A K^+ is represented as a green circle. A box is either occupied by a K^+ or by a water molecule (not shown). The set of boxes on the left represents the 1,3 configuration, and the one on the right represents the 2,4 configuration (see the text). The upper set shows the case when an incoming K^+ pushes the queue of K^+–water–K^+–water (the 1,3 configuration) up one box, to release a K^+ on the opposite side, leading to the 2,4 configuration. The bottom set shows the case when the queue of water–K^+–water–K^+ (the 2,4 configuration) moves up one box, leading to the 1,3 configuration. Figures 1A, 2A–C, and 3A and B were made with Bobscript[13,14] and Raster 3D.[15]

position 4 in the 1,3 configuration or position 1 in the 2,4 configuration) and another ion exits from the opposite side. Thus, conduction would always involve a doubly occupied selectivity filter and be dependent upon strong coupling of ion exit and entry through the queue of ions and water in the filter. This model would predict that a mutation at a single site within the selectivity filter would have consequences for ion occupancy beyond the site mutated.

Site 4 is accessible to alteration by conventional mutagenesis because the intracellular most layer of oxygen atoms in the filter is provided by the side-chain of threonine. Here we investigate the effects of mutating the threonine residue, which directly alters site 4.

Results

Site 4 mutation and the distribution of K^+

Threonine 75 was mutated to cysteine (site 4 mutation) and the structure was solved in the presence of 200 mM KCl and refined to a resolution of 2.2 Å. The cysteine replaces threonine without significantly altering the side-chain volume. Electron density in the selectivity filter is shown (Figure 2A) and compared to the wild-type channel structure determined at 2.0 Å resolution under similar conditions (Figure 2B). In the mutant channel the sulfur atom of the cysteine side-chain takes the position of the γ-carbon of the wild-type threonine side-chain. The result is an almost

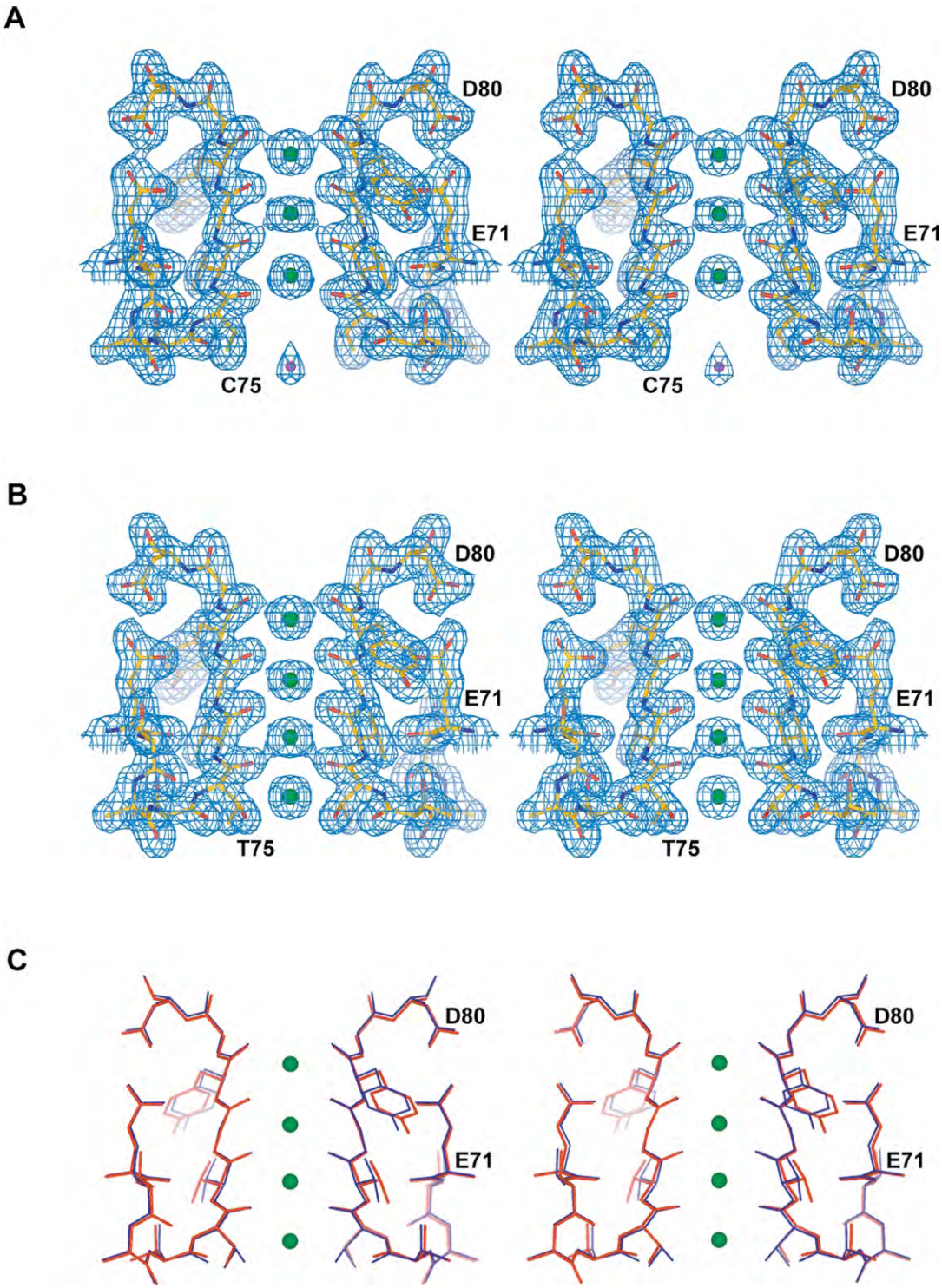

Figure 2. A, Stereo view of the selectivity filter region for the T75C mutant KcsA channel. The structure, solved in 200 mM K^+, is shown with residues E71 to D80 (from two diagonally opposed subunits) rendered in a ball-and-stick representation. Green spheres represent K^+ binding sites in the filter, and the magenta sphere represents a site with residual electron density. The $2F_o - F_c$ electron density map (contoured at 2σ) validating the structure is shown as a blue mesh. B, Stereo view of the selectivity filter region for the wild-type KcsA. The structure (PDB code 1K4C[3]), solved in 200 mM K^+, is represented in the same way as in A. C, Stereo view of the selectivity filter region of the T75C (red) superimposed on that of the wild-type (blue).

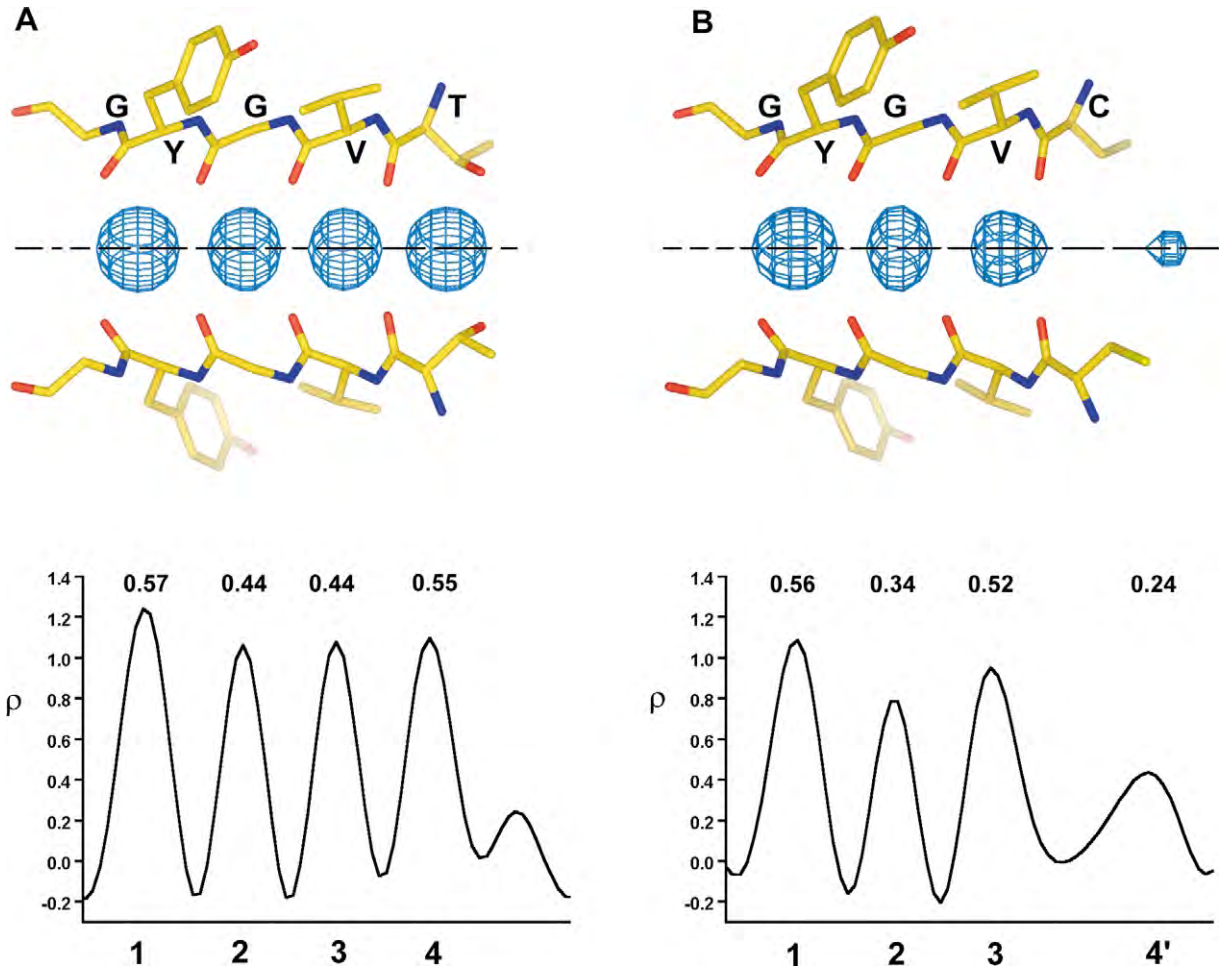

Figure 3. K^+ distributions in the selectivity filter of the wild-type (A) and the T75C (B) KcsA channels. Upper panel: the amino acid residues of the selectivity filter signature sequence (T/CVGYG) are shown in a ball-and-stick representation. $F_o - F_c$ electron density omit maps (contoured at 3σ) validating the four K^+ binding sites are shown as a blue mesh. The left-most site corresponds to site 1 as defined in Figure 1A. The black broken line shows the central axis of the selectivity filter, along which the difference Fourier omit map was sampled to obtain the one-dimensional electron density (ρ), as described in Methods. Lower panel: one-dimensional electron density profiles corresponding to different K^+ binding sites in the selectivity filter. The numbers along the *x*-axis identify the four binding sites as defined in Figure 1A. The number on top of each peak indicates the fractional K^+ occupancy (see Methods).

perfect removal of the threonine hydroxyl with little further perturbation of the channel structure (RMSD for the wild-type and mutant channels from residue 71 to 80 is 0.12 Å) (Figure 2C). Site 4 is rendered incomplete in the mutant channel: where K^+ fits snugly into a cubic cage of eight oxygen atoms surrounding site 4 in the wild-type channel, it experiences a wider almost vestibule-like opening in the mutant channel.

One-dimensional electron density profiles are shown for the wild-type (Figure 3A) and mutant (Figure 3B) channel structures. The areas have been converted into approximate occupancy according the analysis of Zhou & MacKinnon.[1] We emphasize the approximate nature of this measurement and that our conclusions will depend on relative changes rather than precise occupancy values. In the wild-type channel the occupancies of sites 1 and 4 are about 0.55 and of sites 2 and 3 are about 0.45. Interpreted in the context of the two ion filter model described in the Introduction we suppose that the 1,3 and 2,4 configurations each represent about 45% of the channels in the crystal while the remainder (~10%) correspond to a 1,4 configuration (K^+ at sites 1 and 4).[2]

In the mutant channel the electron density profile is altered. Site 4 has a broader and shifted peak with a reduced area consistent with lowered occupancy. The occupancy of site 2 is also somewhat reduced. The apparent "action at a distance", that is, alteration of occupancy at site 2 as a consequence of a mutation at site 4, is easy to understand if ions tend to reside in specific configurations because an energetic alteration of site 4 will affect the occupancy of the 2,4 configuration.

Site 4 mutation and K^+ conduction

The site 4 mutation influences K^+ conduction in KcsA K^+ channels reconstituted into planar lipid

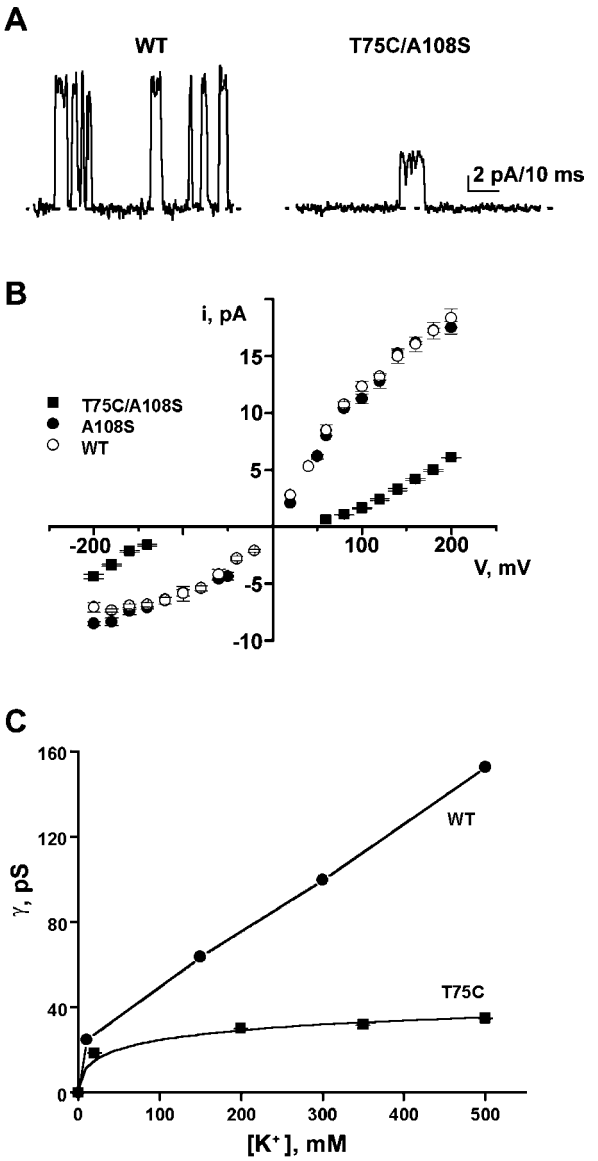

Figure 4. K^+ conduction properties of the T75C/A108S double mutant. A, Single channel recordings of the wild-type (left) and the mutant (right) recorded at 200 mV in symmetrical 200 mM K^+. Broken lines represent closed-state levels. Data were filtered at 1 kHz. B, Single-channel i–V plots in symmetrical 200 mM K^+ for the wild-type (○), the A108S (●), and the T75C/A108S mutant channels (■). C, Cord conductances for the wild-type (180 mV) and the T75C/A108S (200 mV) as a function of K^+ concentration. Data points for the wild-type channel are from Morais-Cabral *et al.*[2] Standard errors are smaller than the width of the points. Curves in Figures 4C, 5, and 6B have no theoretical meaning.

bilayers (Figure 4A). To study conduction in the mutant channel we had to introduce a second mutation that would increase the open probability. The wild-type KcsA K^+ channel normally opens only rarely, and most mutations lower the open probability even further to an immeasurably low level. Heginbotham and co-workers showed that the mutation alanine 108 to serine (located in the inner helix near the channel's gate) increases the open probability of KcsA,[4] and here we use their finding to our advantage to open the site 4 mutant channel. In single channel records it is immediately apparent that the conductance of the double mutant (site 4 and alanine 108 to serine) is smaller than wild-type (Figure 4A). The current-voltage curves in Figure 4B show that the current is reduced over the entire voltage range (−200 mV to +200 mV) and that the reduction is caused by the site 4 mutation: the alanine 108 to serine mutation by itself has no significant influence on conductance compared to the wild-type channel. The qualitative shape of the current-voltage curve is also affected by the site 4 mutation such that the conductance is reduced most dramatically at smaller absolute values of membrane voltage.

The relative reduction of conductance caused by the mutation at site 4 also depends on the K^+ concentration. This effect is shown in Figure 4C, where the conductance γ (current per voltage measured as in Figure 4B) is graphed as a function of the K^+ concentration. At the lowest concentration the mutation causes only a modest reduction compared to wild-type, while at the highest concentration the relative reduction is greatest. The basic shape of the conductance–concentration curve is altered by the mutation in a manner somewhat analogous to the reduction of an enzyme's V_{max}.

Site 4 mutation and Rb^+ conduction

The alkali metal cation Rb^+ conducts, but for most K^+ channels it conducts at lower rates than K^+. This is the case for the KcsA K^+ channel (Figure 5). Moreover, the conductance-concentration curve in Rb^+ is qualitatively similar to what we saw in the site 4 mutant channel in the presence of K^+ (Figure 4C): the conductance "saturates" at a small value. This observation compels us to ask: if Rb^+ conduction through the

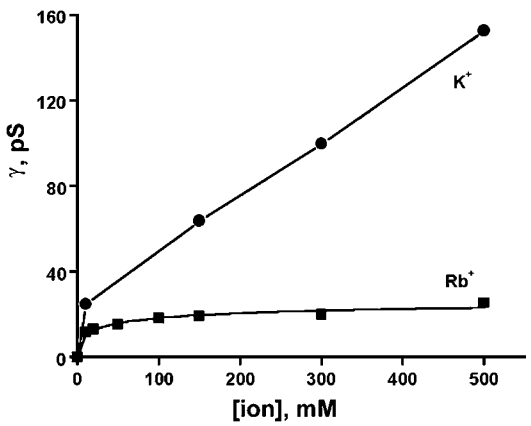

Figure 5. Comparison of K^+ and Rb^+ conduction properties in the wild-type KcsA. Cord conductances (180 mV) are plotted against either K^+ or Rb^+ concentrations. The data in this Figure are from Figure 3(A) of Morais-Cabral *et al.*[2]

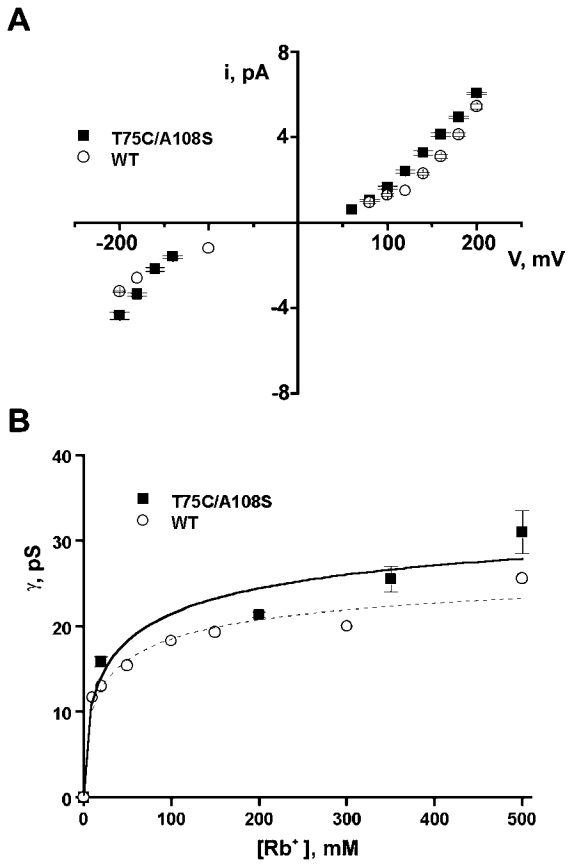

Figure 6. Rb^+ conduction properties in the wild-type and the T75C/A108S. A, Single-channel i–V plots in symmetrical 200 mM Rb^+ for the wild-type (○) and the T75C/A108S (■). B, Cord conductances of the wild-type (180 mV, ○) and the T75C/A108S mutant channels (200 mV, ■) are plotted as a function of Rb^+ concentration.

wild-type channel already looks like K^+ conduction through the site 4 mutant channel, does the mutation have an effect on Rb^+ conduction? We see in Figure 6 that the mutation in this context has little effect: the current-voltage curve (Figure 6A) and the conductance–concentration curve (Figure 6B) are similar for the wild-type and mutant channel when Rb^+ is the current carrier. The mutation that has such a prominent influence on the conduction of K^+ is essentially silent to the conduction of Rb^+.

Discussion

Several lines of experimental evidence support a model for K^+ conduction outlined in Figure 1B. It is well established that the filter contains on average about two K^+ distributed over four ion-binding sites.[1] There is also some evidence that the K ions tend to bind in specific configurations that we call 1,3 and 2,4, with a water molecule hypothesized to reside in between the pair of ions (Figure 1B).[2,3] Some deviation from strictly 1,3 and 2,4 configurations undoubtedly occurs because detailed crystallographic measurements show that the ion occupancy at site 1 does not exactly equal the occupancy at site 3, and sites 2 and 4 are also not exactly equal either.[1] In fact, sites 1 and 4 systematically have a higher occupancy than sites 2 and 3,[1,2] which implies the possible presence of some channels with a 1,4 configuration, a K^+ in 1 and 4 with two water molecules in between.[2] To a first approximation, however, the data are in good agreement with the filter being predominantly (~90%) in either the 1,3 or 2,4 configurations when crystals are equilibrated with more than 20 mM K^+. These configurations have led us to formulate the model for conduction (Figure 1B).[2]

Specific configurations of ions in the filter make simple predictions about the way K^+ ions will distribute in the filter if a single site is altered by mutation. Here we investigate what happens when site 4 is mutated. We observe that the occupancy of site 4 is reduced, as is the occupancy of site 2, while sites 1 and 3 remain essentially unaltered. This observation lends very strong support for the proposal of 1,3 and 2,4 configurations of ions in the filter. In fact, it is not easy to explain the result in any other way. This basic observation is the most important result here.

We studied certain electrophysiological properties of the site 4 mutant channel and found that its conductance in K^+ is reduced. To a "zeroth-order" approximation we offer the following explanation for this effect. If one simulates ions hopping around the cycle in Figure 1B it is easy to show that conductance is maximized when the energy difference between the 1,3 and 2,4 configurations is zero.[2] In the wild-type channel the 1,3 and 2,4 configurations are nearly equally represented in the crystal because occupancy at 1 and 3 is roughly the same as at 2 and 4. These configurations must therefore be energetically equivalent. The energetic balance is disturbed in the mutant: the occupancy of the 2,4 configuration is less than the 1,3 configuration. Because of the energy difference between them we should expect, all else being equal, a reduction in conductance. Even the relatively greater reduction at high concentrations of K^+ (Figure 4C) can be explained qualitatively in terms of an energy difference between the configurations because an energy difference necessitates an energy step in going around the cycle: at high K^+ concentrations when ion entry is fast, the internal hopping transition (bottom pathway, Figure 1B) eventually becomes rate-limiting, just as product dissociation becomes rate-limiting at high substrate concentrations in a Michaelis–Menten enzyme.[5]

We emphasize zeroth-order in the above explanation of the reduced conductance for several reasons, the most important being that the apparent energy difference between 1,3 and 2,4 configurations in the mutant channel is small, corresponding to much less than 1.0 kcal mol^{-1} estimated by applying the occupancies to the Boltzmann distribution. Even a small energy

difference should reduce the conductance somewhat, but probably not to the extent that we observe. But careful inspection of the data tells us that the mutation does not simply shift the equilibrium distribution from 2,4 to 1,3, and that the energy difference between these configurations is not the entire story. The mutation actually reduces the total occupancy of the filter to less than two ions (~1.7 ions) on average by lowering the occupancy of the 2,4 configuration, without changing the 1,3 configuration much. The reduction of occupancy means that a more quantitative analysis would require us to consider ion configurations (kinetic states) outside the cycle (Figure 1B). We have carried out such calculations using more complicated kinetic networks to relate occupancy to conduction,[2] but these calculations have not given us deeper insight into the conduction mechanism.

Rubidium conduction through K^+ channels has been studied extensively. In most K^+ channels, including KcsA, Rb^+ conducts less well than K^+ with a reduced conductance especially at high concentrations, as shown (Figure 5). In crystallographic experiments Rb^+ binds at only three positions in the filter, near the K^+ sites 1, 3 and 4, consistent with a combination of 1,3 and 1,4 configurations.[1,2] Based on the crystallographic data we have proposed that the reduced Rb^+ conductance is related to the lack of balanced 1,3 and 2,4 configurations as is seen for K^+.[2] It is now interesting to see that the site 4 mutation has almost no effect on Rb^+ conduction. Qualitatively, this observation is in keeping with the idea that very high rates are achieved in the case of K^+ because of its "energetically balanced" conduction cycle.

Methods

Protein purification and crystal preparation

The T75C mutant KcsA in complex with antibody Fab fragments was purified as described.[3,6] Crystals (~25 μm × 30 μm × 200 μm) of space group *I*4 appeared seven to 15 days after equilibrating a 1 : 1 mixture of the protein (~9 mg/ml) and the reservoir solution (18–25% (w/v) PEG400, 50 mM magnesium acetate, 50 mM sodium acetate at pH 5.4 or 5.6) against the reservoir using the sitting-drop method (20 °C). Cryo-protection of the crystals was achieved through vapor-diffusion by increasing the concentration of PEG400 in the reservoir to 40%, in steps of 5% per day. The crystals were frozen in liquid nitrogen-cooled liquid propane.

Cystallographic analysis

Data were collected at beam line X25 at the National Synchrotron Light Source (Brookhaven National Laboratory) (Table 1). The data were processed and scaled with Denzo and Scalepack from the HKL program suite[7] and the CCP4 package.[8] The wild-type coordinates (PDB code 1K4C[3]), with the threonine 75 replaced by an alanine, were used to calculate the initial electron density map, and the electron density corresponding to the S^γ of the cysteine 75 was unambiguously identified in the map. The model was refined by several cycles of manual rebuilding in the program O,[9] and simulated annealing, energy minimization and individual *B*-factor refinement using CNS.[10]

One-dimensional electron density profiles were obtained as described.[1,2] Briefly, the data set for the mutant (30–2.2 Å) was scaled to the wild-type KcsA data set (1K4C). An $F_o - F_c$ omit map was calculated using the refined model, with ions and the selectivity filter residues (CVGYG) removed. The one-dimensional electron density profile was obtained by sampling the omit map along the central axis of the selectivity filter, using MAPMAN.[11] It was reported[1] that removing the selectivity filter residues for map calculation causes only small changes in the model phases, but can significantly reduce local errors in the selectivity filter region of the electron density map. K^+ occupancy for each site was estimated from the relative peak areas of the one-dimensional electron density profile.[1] The fractional occupancy of each site in the wild-type is slightly different from that reported,[1] due to truncation of the data set to 2.2 Å.

Electrophysiology

The wild-type and the mutant KcsA channels were purified on a Talon Co^{2+}-affinity column as described.[3,6] The His-tag was removed by thrombin digestion, and channels were further purified by gel filtration and reconstituted into lipid vesicles (10 mg/ml) as described.[12] The final protein-to-lipid ratio was ~5 μg/mg for the wild-type and the A108S mutant. Planar lipid bilayers of 1-palmitoyl-2-oleoyl-*sn*-glycero-3-phosphoethanolamine (15 mg/ml) and 1-palmitoyl-2-oleoyl-*sn*-glycerol-3-[phospho-rac-(1-glycerol)] (5 mg/ml) in decane were painted over a 50 micrometer hole in a plastic partition. To increase the chance of observing channel activities for the T75C/A108S, the double

Table 1. Data collection and refinement statistics

Space group	Unit cell (Å)	Resolution (Å)	Total/unique no. of reflections	Redundancy[a]
*I*4	$a = 154.71$, $c = 75.93$	30–2.2	405,120/45,872	8.8
I/σ	Completeness (%)	R_{sym}[b]	r.m.s.d[c]	R_{free}/R_{work} (%)[d]
27 (3.7)	99.7(98.1)	0.057(0.288)	1.3°/0.006 Å	24.3/22.4

Numbers in parentheses are statistics for the last resolution shell.
[a] Redundancy represents the ratio of the total number of measurements to the number of unique reflections.
[b] $R_{sym} = \sum|I_i - \langle I_i\rangle|/\sum I_i$, where $\langle I_i\rangle$ is the average intensity of symmetry-equivalent reflections.
[c] r.m.s.d of bond is the root-mean-square deviation of bond angle and length.
[d] $R = \sum|F_o - F_c|/\sum F_o$; 5% of the data that were excluded in the refinement were used in the R_{free} calculation.

mutant was reconstituted at ~60 μg/mg protein-to-lipid ratio to increase the average number of channels per vesicle. To increase vesicle fusion with the lipid bilayer, KCl was added to the vesicle suspension to achieve the final salt concentration of ~1.2 M immediately prior to the experiment and the mixture was sonicated for ten seconds. Single-channel currents were measured using an Axon 200B patch-clamp amplifier (Axon Instruments), filtered at 2 kHz (−3 dB, Frequency Device) (1 kHz for display in Figure 4A), digitized at 10 kHz (DigiData 1200, Axon Instruments) and recorded on a computer. External solutions contained the KCl concentration specified in the text, and 10 mM Hepes (pH 7.0); internal solutions contained in addition to KCl, 10 mM succinate (pH 4.0).

Atomic coordinates

The atomic coordinates and structure factors for the T75C mutant KcsA channel are deposited with the Protein Data Bank under the PDB code 1S5H.

Acknowledgements

We thank the staff at the National Synchrotron Light Source X-25 station for assistance, Y. Zhou and F. Valiyaveetil for help during various stages of this project, and Q. Jiang, S. Lee and S. Lockless for advice on the manuscript. This project was supported by a grant from the National Institutes of Health to R.M. (GM47400). R.M. is an investigator in the Howard Hughes Medical Institute.

References

1. Zhou, Y. & MacKinnon, R. (2003). The occupancy of ions in the K^+ selectivity filter: charge balance and coupling of ion-binding to a protein conformational change underlie high conduction rates. *J. Mol. Biol.* **333**, 965–975.
2. Morais-Cabral, J. H., Zhou, Y. & MacKinnon, R. (2001). Energetic optimization of ion conduction rate by the K^+ selectivity filter. *Nature*, **414**, 37–42.
3. Zhou, Y., Morais-Cabral, J. H., Kaufman, A. & MacKinnon, R. (2001). Chemistry of ion coordination and hydration revealed by a K^+ channel-Fab complex at 2.0 Å resolution. *Nature*, **414**, 43–48.
4. Irizarry, S. N., Kutluay, E., Drews, G., Hart, S. J. & Heginbotham, L. (2002). Opening the KcsA K^+ channel: tryptophan scanning and complementation analysis lead to mutants with altered gating. *Biochemistry*, **41**, 13653–13662.
5. Nelson, D. L., Lehninger, A. L. & Cox, M. M. (2000). *Lehninger Principles of Biochemistry*, Worth Publishing, New York.
6. Doyle, D. A., Morais, C. J., Pfuetzner, R. A., Kuo, A., Gulbis, J. M., Cohen, S. L. *et al.* (1998). The structure of the potassium channel: molecular basis of K^+ conduction and selectivity. *Science*, **280**, 69–77.
7. Otwinowski, Z. & Minor, W. (1997). Processing of X-ray diffraction data collected in oscillation mode. *Methods Enzymol.* **276**, 307–326.
8. Collaborative Computational Project number 4 (1994). The CCP4 suite: programs for protein cystallography. *Acta Crystallog. sect. D*, **50**, 760–763.
9. Jones, T. A., Zou, J. Y., Cowan, S. W. & Kjeldgaard, M. (1991). Improved methods for building protein models in electron density maps and the location of errors in these models. *Acta Crystallog. sect. A*, **47**, 110–119.
10. Brunger, A. T., Adams, P. D., Clore, G. M., DeLano, W. L., Gros, P., Grosse-Kunstleve, R. W. *et al.* (1998). Crystallography NMR system: a new software suite for macromolecular structure determination. *Acta Crystallog. sect. D*, **54**, 905–921.
11. Kleywegt, G. J. & Jones, T. A. (1996). xdlMAPMAN and xdlDATAMAN—programs for reformatting, analysis and manipulation of biomacromolecular electron-density maps and reflection data sets. *Acta Crystallog. sect. D*, **52**, 826–828.
12. Heginbotham, L., LeMasurier, M., Kolmakova-Partensky, L. & Miller, C. (1999). Single streptomyces lividans K^+ channels: functional asymmetries and sidedness of proton activation. *J. Gen. Physiol.* **114**, 551–560.
13. Kraulis, P. J. (1991). MOLSCRIPT: a program to produce both detailed and schematic plots of protein structures. *J. Appl. Crystallog.* **24**, 946–950.
14. Esnouf, R. M. (1999). Further additions to MolScript version 1.4, including reading and contouring of electron-density maps. *Acta Crystallog. sect. D*, **55**, 938–940.
15. Merritt, E. A. & Bacon, D. J. (1997). Raster3D: photorealistic molecular graphics. *Methods Enzymol.* **277**, 505–524.

Edited by D. Rees

(Received 22 January 2004; received in revised form 5 March 2004; accepted 8 March 2004)